REPORT DOCUMENTATION PAGE

AFRL-SR-BL-TR-02-

0241

1. AGENCY USE ONLY (Leave blank)	2. REPORT DATE	3. REPORT TYPE AND DATES COVERED
	04 June 2001	Final Technical 01Mar1998-28Feb2001

4. TITLE AND SUBTITLE

Biomarkers for Detection of In Vitro Ocular Irritancy

5. FUNDING NUMBERS

Grant
F49620-98-1-0292

61102F

2312/AX

6. AUTHOR(S)

Thomas E. Eurell, D.V.M., Ph.D., Dipl. A.B.T.
Department of Veterinary Biosciences

7. PERFORMING ORGANIZATION NAME(S) AND ADDRESS(ES)

The Board of Trustees of the University of Illinois
c/o Grants and Contracts Office, 109 Coble Hall
801 S. Wright St.
Champaign, IL 61820

8. PERFORMING ORGANIZATION REPORT NUMBER

9. SPONSORING / MONITORING AGENCY NAME(S) AND ADDRESS(ES)

AFOSR/NL
801 Randolph St, Room 732
Arlington, VA 22203-1977

10. SPONSORING / MONITORING AGENCY REPORT NUMBER

20020215 100

11. SUPPLEMENTARY NOTES

12a. DISTRIBUTION / AVAILABILITY STATEMENT

DISTRIBUTION STATEMENT A
Approved for Public Release
Distribution Unlimited

AIR FORCE OFFICE OF SCIENTIFIC RESEARCH (AFOSR)
NOTICE OF TRANSMITTAL DTIC. THIS TECHNICAL REPORT
HAS BEEN REVIEWED AND IS APPROVED FOR PUBLIC RELEASE
LAW AFR 190-12. DISTRIBUTION IS UNLIMITED.

12b. DISTRIBUTION CODE

13. ABSTRACT *(Maximum 200 Words)*

Exposure of rabbit corneas to nanosecond pulse width 1540 nm infrared laser light produced a less severe coagulative necrosis when compared to millisecond pulse width exposures. We expected this result because nanosecond pulse widths should have less of a photothermal effect than millisecond pulse widths. Matrix Metalloproteinase-2 (MMP-2) immunohistochemistry was used to detect if subtle stromal remodeling had occurred. We found a markedly increased MMP-2 immunohistochemical pattern than what we would have predicted from the H&E stains alone. Approximately half of the beam path was filled with MMP-2 reaction product. As far as we know this is the first analysis comparing the stromal remodeling effects of an infrared laser operating in both the millisecond and nanosecond pulse widths. This finding is important to the AFOSR mission because it demonstrates that significant tissue changes associated with corneal wound healing can occur following exposure to nanosecond laser pulse widths that are not detectable with standard histologic techniques.

14. SUBJECT TERMS	15. NUMBER OF PAGES
In Vitro, Ocular Irritancy, Biomarkers, Laser	12
	16. PRICE CODE

17. SECURITY CLASSIFICATION OF REPORT	18. SECURITY CLASSIFICATION OF THIS PAGE	19. SECURITY CLASSIFICATION OF ABSTRACT	20. LIMITATION OF ABSTRACT
Unclassified	Unclassified	Unclassified	

Biomarkers for Detection of *In Vitro* Ocular Irritancy

AFOSR Grant # F49620-98-1-0292

Final Technical Report (March 1, 1998- February 28, 2001)

Prepared by

Thomas E. Eurell, D.V.M., Ph.D., Dipl. A.B.T.

Department of Veterinary Biosciences

College of Veterinary Medicine

University of Illinois

May 2001

Executive Summary

In an effort to identify mechanistically based biomarkers of ocular irritation, we conducted studies to detect the presence of cytochrome p450 (CYP) enzymes in native human and rabbit corneas and organotypic corneal equivalents. Using reverse transcriptase-polymerase chain reaction (RT-PCR) methods, we detected significant increases in the messenger RNA (mRNA) for CYP2B. Although little information is available about the presence or activity of biotransformation enzymes such as CYP in the cornea, they may be important to humans in dealing with oxidizing pollutants such as smog. This theory may suggest a new avenue of investigation for U.S. Air Force chemicals that have volatile or aerosol components capable of ocular exposure (fuels, hydraulic fluids, and possibly deicing compounds). The presence of biotransformation enzymes in the cornea would expand the perspective of ocular risk assessment beyond direct irritation or erosion to include the eye as a potential target tissue.

During the first year of this project, an opportunity arose to initiate a new series of collaborations with scientists at Brooks Air Force Base (Dr. B. Rockwell), the Uniformed Services University of the Health Sciences (Drs. P. Roach and T. Johnson) and the U.S. Air Force Academy (Dr. J. Obringer) in regards to laser effects on ocular tissues. Our focus in these collaborations was the isolation and culture of retinal-pigmented epithelium (RPE), the development of methods for explant culture of porcine and rabbit ocular tissues and the investigation of tissue effects following laser exposure. In an effort to continue the work on the biotransformation enzymes of the cornea and extend investigations into the area of laser-ocular tissue interaction we streamlined our efforts. Total RNA from human and rabbit corneal specimens were prepared and stored for future RT-PCR analysis and our efforts were focused on laser-ocular tissue interactions.

We supported research projects on laser-ocular tissue interaction by supplying rabbit and pig ocular tissue for laser exposure and conducting post-exposure histopathologic and biochemical analysis of the tissue response. The data obtained from this collaboration was presented at the SPIE Photonics meeting in January 2001 (San Jose, CA) and served as preliminary data for an R01 application to the National Eye Institute. Recent studies by our research group have discovered a relationship between the pulse width of infrared laser light (1540nm) and the degree of post-exposure corneal wound healing. Exposure of rabbit corneas to nanosecond pulse width 1540 nm infrared laser light produced a less severe coagulative necrosis when compared to millisecond pulse width exposures. We expected this result because nanosecond pulse widths should have less of a photothermal effect than millisecond pulse widths. However, we used Matrix Metalloproteinase-2 (MMP-2) immunohistochemistry to detect if subtle stromal remodeling had occurred. We were surprised to find a markedly increased MMP-2 immunohistochemical pattern than what we would have predicted from the H&E stains alone. Approximately half of the beam path was filled with MMP-2 reaction product. As far as we know this is the first analysis comparing the stromal remodeling effects of an infrared laser operating in both the millisecond and nanosecond pulse widths. In order to address subtle differences in post-exposure, corneal MMP-2 immunohistochemistry reaction products, we developed specific sub-routines in our image analysis program to obtain quantitative information. We are currently developing analysis methods to include both the linear and area measurements and densitometry data into a single "lesion score". This finding is important to the AFOSR mission because it demonstrates that significant tissue changes associated with wound healing can occur in the cornea following exposure to nanosecond pulse widths that are not detectable using standard histologic techniques.

Introduction

This research project was designed to investigate potential biomarkers for *in vitro* detection of ocular irritancy. We conducted studies to detect the presence of cytochrome p450 (CYP) biotransformation enzymes in human and rabbit corneas using reverse transcriptase-polymerase chain reaction (RT-PCR) methods. The presence of biotransformation enzymes in the cornea would expand the perspective of ocular risk assessment beyond direct irritation or erosion to include the eye as a potential target tissue.

During the first year of this project, we started a new series of collaborations with scientists at Brooks Air Force Base (Dr. B. Rockwell), the Uniformed Services University of the Health Sciences (Drs. P. Roach and T. Johnson) and the U.S. Air Force Academy (Dr. J. Obringer) in order to investigate biomarkers of laser effects on ocular tissues. Our focus in these collaborations was the isolation and culture of retinal-pigmented epithelium (RPE), the development of methods for explant culture of porcine and rabbit ocular tissues and the investigation of tissue effects following laser exposure. We received a significant decrease in funds available for this research at the beginning of year 2. In an effort to continue the work on the biotransformation enzymes of the cornea and extend investigations into the area of laser-ocular tissue interaction we streamlined our efforts. Total RNA from human and rabbit corneal specimens were prepared and stored for future RT-PCR analysis and our efforts were focused on laser-ocular tissue interactions.

We supported research projects on laser-ocular tissue interaction by supplying rabbit and pig ocular tissue for laser exposure and conducting post-exposure histopathologic and biochemical analysis of the tissue response. An important aspect of this project was the production of *in vitro*, organotypic corneal models. Our research team has developed three dimensional, *in vitro* organotypic models for the rabbit and human anterior cornea that we believe will provide the information necessary to address the problems of species extrapolation and assay validation. The organotypic corneal models (corneal equivalents) consist of a collagen-based stromal matrix that contains corneal keratocytes and epithelial cells from the respective host species. The resulting three-dimensional models are histologically and biochemically analogous to their respective native tissues. This approach maximizes the potential for a good correlation between *in vitro* test results and the extrapolation of experimental data to human experience. Using methods outlined in this report, one rabbit cornea provided enough seed culture cells to produce 40-50 rabbit organotypic corneal equivalents. Human corneal tissue provided enough seed culture cells to produce 3-5 human organotypic corneal equivalents. No live animals were used in this research project as we obtained the rabbit eyes from a meat processing plant. Human corneal tissue was recovered from post-surgical specimens obtained from a local hospital.

The principal objectives of this study were:

(1) Investigate the occurrence of specific isoforms of CYP (CYP1A, CYP2B, CYP3A and CYP4A) using RT-PCR methods in both human and rabbit corneas.
(2) Produce organotypic corneal equivalents for the pig, rabbit and human cornea.
(3) Develop methods for the culture of porcine and rabbit retinal-pigmented epithelial cells and explant ocular tissues.
(4) Conduct studies to obtain biomarker data for laser-ocular tissue interaction.

This final technical report represents our efforts from March 1, 1998- February 28, 2001.

USAF Relevancy

The USAF has a scientific mission and a congressional mandate to reduce the number of animals used in research and to protect USAF personnel from operational hazards. The use of *in vitro* methods to screen USAF compounds of interest and operational procedures (laser) is an important component of the AFOSR Predictive Toxicology Program. The transfer of organotypic model technology from our laboratory to the laboratories at Brooks AFB (Dr. Ben Rockwell) and the Uniformed Services University of the Health Sciences (Drs. Roach and Johnson) should provide USAF scientists with useful methods that are directly applicable to the AFOSR Predictive Toxicology Program.

Technical Background

Objective 1- Investigate the occurrence of specific isoforms of CYP (CYP1A, CYP2B, CYP3A and CYP4A) using RT-PCR methods in both human and rabbit corneas.

The RNA present in the native human and rabbit corneas, or the corneal equivalents was harvested using commercial isolation reagents (RNA Stat-60, Leedo Medical) and incubated with reverse transcriptase (ProMega, Inc.) to yield DNA. The upstream and downstream primers for the human and rabbit CYP450 isoforms (CYP1A, CYP2B, CYP2E, CPY3A) polymerase chain reaction were incubated through approximately 25-30 thermal cycles to produce a sufficient amount of DNA for electrophoretic analysis. Cyclophilin (ProMega, Inc.) was used as a loading control and standard genetic marker in all experiments. The above four CYP450 isoforms were selected because of the availability of PCR primers and their reported occurrence in extrahepatic tissues.

Objective 2- Produce organotypic corneal equivalents for the pig, rabbit and human cornea.

Cultures of corneal epithelial cells and keratocytes from native human, rabbit and pig corneal specimens served as the seed cultures for the organotypic corneal equivalents. Corneal equivalents were produced in two steps. First, a liquid collagen/corneal keratocyte seed culture suspension was added to a Transwell (Costar) polycarbonate tissue culture insert contained within a 12 well tissue culture plate. The polycarbonate membrane of the insert served as a platform for the gelatinization of the stromal collagen and the growth of stromal keratocytes. The collagen/ keratocyte suspension formed a gel during incubation (37°C, 5% CO_2) and the keratocytes were grown in culture for 3-5 days. Second, a seed culture suspension of corneal epithelial cells was plated upon the collagen/ keratocyte gel and grown in culture for an additional 5-7 days. The tissue culture fluid level was slowly lowered over the incubation period until an epithelial cell-air interface was established. Corneal equivalents were used for experimental laser exposures after 2-4 days of an air interface.

Objective 3- Develop methods for the culture of porcine and rabbit retinal-pigmented epithelial (RPE) cells and explant ocular tissues.

Porcine and rabbit eyes were obtained within 2 hours of death from a local abattoir. The anterior segment of the eye, vitreous humor and neural retina were removed by gentle manipulation and aspiration. The resulting eyecup was then gently rinsed with Hanks Balanced Salt Solution (HBSS) to remove neural retinal remnants from the RPE layer. Two milliliters of HBSS, that contained 0.25% Trypsin + 0.1% EDTA, was added to the eyecup containing the RPE layer and was then incubated at 37°C for 20 minutes. Enzymatic activity was stopped by rinsing the eyecup three consecutive times with Dulbecco's Modified Eagles Medium (DMEM) containing 10% fetal bovine serum. RPE cells released

by the enzymatic activity were collected from the 3 rinses of the eyecup and the cell suspensions were transferred to a 50ml centrifuge tube containing an equal volume of DMEM + 10% fetal bovine serum. The cell suspension was then centrifuged at 150xG for 5 minutes at room temperature. The supernatant was discarded and the cell pellet resuspended in 1ml DMEM supplemented with 10% NU-Serum (Collaborative Biomedical, Bedford, MA), 2mM L-glutamine and 1% antibiotic/antimycotic solution. Purified RPE cells were obtained using differential sedimentation by placing a 1 ml RPE cell suspension on top of 12 ml of Lymphoprep (NycoMed, Oslo, Norway) and allowing gravity sedimentation for 20 minutes at room temperature. RPE cells were recovered from the middle sedimentation band by aspiration, rinsed in 10 ml of supplemented DMEM, and then centrifuged at 150xG for 5 minutes at room temperature. The cell pellet was resuspended in 1ml of supplemented DMEM and RPE cell number and viability were determined by hemacytometer count and lack of staining with trypan blue.

Our research team developed a new approach to the culture of RPE cells using a self-forming alginate bead matrix. Keltone-LVCR (Kelco, San Diego, CA) alginate powder was used to make a 1.2-% aqueous alginate solution that was filter sterilized prior to cell culture. RPE cells isolated as described above were suspended in a 1.2-% alginate solution (1:10 dilution) and passed in a drop wise fashion through a 25-gauge needle, at a height of 10 cm, into a 102mM $CaCl_2$ solution. The alginate drops gelled and formed a bead immediately upon entering the $CaCl_2$ solution. Alginate beads containing RPE cells were allowed to polymerize for 10 minutes in the $CaCl_2$ solution and then washed 3 times in supplemented DMEM. Digital images of RPE cells were taken at each media change to monitor cell morphology and pigmentation.

Objective 4- Conduct studies to obtain biomarker data for laser-ocular tissue interaction.

Laser Exposures: All laser exposures were single pulse, 1540 nm laser light. Millisecond exposures were set at 0.8 millisecond pulse widths with a 0.6-micron diameter spot size and a calculated energy density of 100 J/cm^2 at 1/e^2. Nanosecond exposures were set at 500 nanosecond pulse widths with a 0.3-micron diameter spot size and a calculated energy density of 40 J/cm^2 at 1/e^2. The laser used in corneal exposures was manufactured by Laser Sight Technologies (Winter Park, FL). It had an Erbium:Glass rod and q-switched circuitry to produce pulse widths in the ms-ns range at a wavelength of 1540 nm. The pulse widths were measured using a Germanium detector (Thor Labs PDA 255) connected to a TDS 644B-digitizing oscilloscope (Tektronix). Energy measurements were made with a EPM 2000 detector (Molectron) connected to a J-25 energy probe (Molectron).

Histomorphometry: Digital images of the corneas were obtained (Kodak EDAS system), the tissues were frozen in OCT embedding medium (Tissue-Tek) and frozen sections were taken using a motorized cryomicrotome (Bright Instruments). Using the digital images of the post-exposure corneas projected onto a measuring grid, we could accurately locate the relative position of the circular laser lesion in the embedded tissue. Phase differential interference contrast microscopy (BK-2 microscope, Olympus) was used to evaluate unstained sections for relative position within the lesion, as well as, proper orientation and the occurrence of any sectioning artifacts. This allowed us to section through the lesion with micrometer precision and accurately resolve the inside edge, middle and outside edge of the laser lesion. All tissue sections for histomorphometric analysis of laser effects were taken through the middle of the lesion. Images of histologic sections were obtained using a Leitz Orthoplan microscope equipped with a SpotRT digital camera (Diagnostic Instruments). Alterations in the epithelial parameters (e.g., area of hyaline coagulative change vs. area of granular coagulative change) and stromal parameters (e.g., area of coagulative necrosis, number and distribution of keratocytes) were evaluated between millisecond and nanosecond treatment groups.

Immunohistochemical Analysis of Laser Exposed Tissue: Immunohistochemistry procedures were performed in CoverPlate Immunostaining Chambers (Shandon Scientific). Indirect immunostaining for matrix metalloproteinase 2 (MMP-2) was performed using mouse monoclonal antibodies (clone 42-5D11). Checkerboard titrations of primary mouse monoclonal antibodies and secondary biotinylated goat anti-mouse IgG (Vector Labs) was used to establish appropriate dilutions of primary and secondary reagents. The Vectastain Elite ABC kit (Vector Labs) was used for immunohistochemical analysis, which was conducted following manufacturer's recommended procedures. Quantitative evaluations of the MMP-2 diaminobenzidine (DAB) immunohistochemical reaction products in the corneal epithelial and stromal layers were performed using Image Pro Plus analysis software (Media Cybernetics).

Summary of Accomplishments and Significance of Research Project

Human and rabbit native corneas appear to have different CYP450 isoform mRNA profiles (Table 1). This may be important in regards to extrapolation of experimental data from the rabbit to human experience. A human corneal disease (Fuch's Dystrophy) is often a cause of corneal transplantation and is a common finding in the tissue samples obtained for this research project. Comparison of Fuch's dystrophy corneal tissue to normal human corneal tissue revealed that CYP2B and CYP4A are very highly expressed in this disease, whereas, CYP1A is moderately increased and CYP3A4 is significantly decreased (Table 1). These studies have the potential to elucidate the role of corneal biotransformation enzymes in the tissue response to ocular irritants as well as important disease conditions. A particularly important question would be if chronic, low-level toxic injury to the cornea could predispose the individual to corneal disease. Reference values for corneal equivalent CYP will provide a method to further validate extrapolation of data from *in vitro* corneal equivalent exposures to *in vivo* data. One advantage of this approach is that we can evaluate the CYP composition of the seed cultures (epithelial and stromal cells) and determine the source of CYP activity in the corneal equivalents. This data will provide a unique tool to explore the source of CYP activity in the native human and rabbit corneal tissue.

Table 1. Mean relative amount of native corneal mRNA for CYP isoforms. The PCR reaction was standardized using the housekeeping gene Cyclophilin (Cyc) and the data reported as the amount relative to a Cyc value of 1.0. The data represents the mean relative amounts of the indicated CYP isoforms for 10 human and 6 rabbit corneas.

Corneal Tissue Sample (n)	Mean (± 1 SD) Relative Amount CYP mRNA			
	1A1	2B6	3A4	4A
Rabbit-Normal (6)	44.1 (5.8)	1.1 (0.2)	99.8 (12.1)	10.2 (1.1)
Human-Normal (2)	2.3 (0.5)	1.5 (0.2)	728.3 (74.3)	2.0 (0.4)
Human-Edema (4)	1.8 (0.5)	1.0 (0.2)	770.6 (12.0)	1.4 (0.5)
Human-Fuch's (4)	24.1 (4.1)	646.7 (28.7)	428.2 (36.9)	176.2 (22.8)

Drs. Roach and Johnson developed a laser alignment and targeting system for the explant tissues and corneal equivalents that allowed us to reliably locate areas of tissue laser exposure. Using digital images of the post-exposure corneas projected onto a measuring grid, we could accurately locate the

relative position of the circular laser lesion in the embedded tissue. This allowed us to section through the lesion with micrometer precision and accurately resolve the inside edge, middle and outside edge of the laser lesion. All tissue sections used for morphometric analysis were taken through the middle of the lesion. This was a critical accomplishment in order to reproducibly obtain comparative histopathologic and biochemical data.

Representative Histomorphometry Data for Pig and Rabbit Corneas

Table 2. Reference Histomorphometric Data from Thirty Control Areas in Pig and Rabbit Corneas.

Species	Epithelial Thickness (μ) (mean ±1 S.D.)	Stromal Thickness (μ) (mean ±1 S.D.)	Total Corneal Thickness (μ) (mean ±1 S.D.)
Pig	66.7±9.7	1,198.8±98.8	1,264.4±103.7
Rabbit	36.0±2.6	623.1±37.4	657.9±36.1

Table 3. Histomorphometric Data of Lesions from Six Pig Corneas in Relation to Different Laser Exposure Conditions.

Spot Size (cm^2)	Energy Density (J/cm^2 at area $1/e^2$)	Maximum Depth of Lesion (microns)	Total Area of Lesion ($microns^2$)
0.00047	474	1,180	282,357
0.00047	440	919	274,474
0.00047	435	910	235,445
0.00201	108	645	191,479
0.00201	97	206	129,437
0.00201	65	85	64,397

Table 4. Histomorphometric Data of Lesions from Three Rabbit Corneas in Relation to Different Laser Exposure Conditions.

Spot Size (cm^2)	Energy Density (J/cm^2 at area $1/e^2$)	Maximum Depth of Lesion (microns)	Total Area of Lesion ($microns^2$)
0.00047	456	712	249,148
0.00047	452	660	221,717
0.00047	444	623	218,449

Single pulse, 1540 nm laser light with a pulse width of 1 microsecond altered the morphologic appearance of explant rabbit and pig corneas following *ex vivo* exposure (Figures 1 and 2). Several features of the response to laser exposure may reflect species-specific tissue differences. The rabbit corneal epithelium showed a homogeneous coagulative necrosis with a distinct demarcation between necrotic and normal epithelium (Figure 1). The pig epithelium also showed a distinct demarcation

between necrotic and normal epithelium (Figure 2), however, there were several remarkable differences in the tissue response between the two species including coagulative necrosis pattern and nuclear morphology. These changes suggested a different and less severe response of the pig epithelium to the laser light when compared to the rabbit epithelium

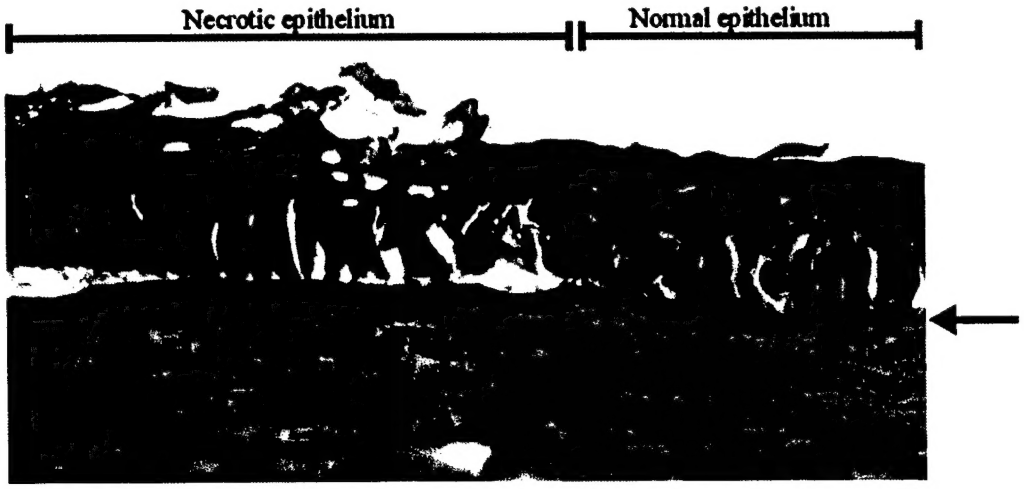

Figure 1. Frozen Section of a Rabbit Anterior Cornea at the Epithelial-Stromal Junction. Arrow indicates the basement membrane; (*) is coagulated stromal collagen. Note separation of epithelial-stromal layers at basement membrane directly underneath necrotic epithelium. Original magnification=400x, H&E stain.

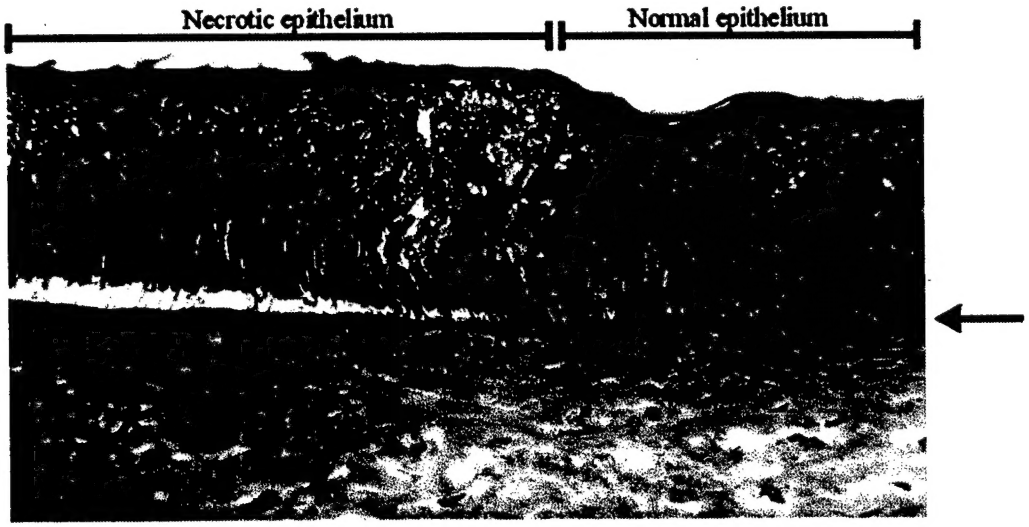

Figure 2. Frozen Section of a Pig Anterior Cornea at the Epithelial-Stromal Junction. Arrow indicates the basement membrane; (*) is coagulated stromal collagen. Note separation of epithelial-stromal layers at basement membrane directly underneath necrotic epithelium. The epithelial basement membrane of the pig is characteristically more prominent than the rabbit (Figure 1). Original magnification=400x, H&E stain.

One feature of this difference that may be particularly important is the shape of the corneal stromal lesion. The area of the stromal lesion at the lesion surface is very similar between the species and reflects the spot size of the laser beam. However, the pig corneal stromal lesion quickly narrows as

it moves deeper into the stroma (Figure 3) compared to the rabbit corneal stromal lesion, which maintains a relatively constant width throughout the stroma. This difference suggests that features of the pig cornea may induce a "tissue focusing" of the laser beam to a significantly greater extent than the rabbit cornea.

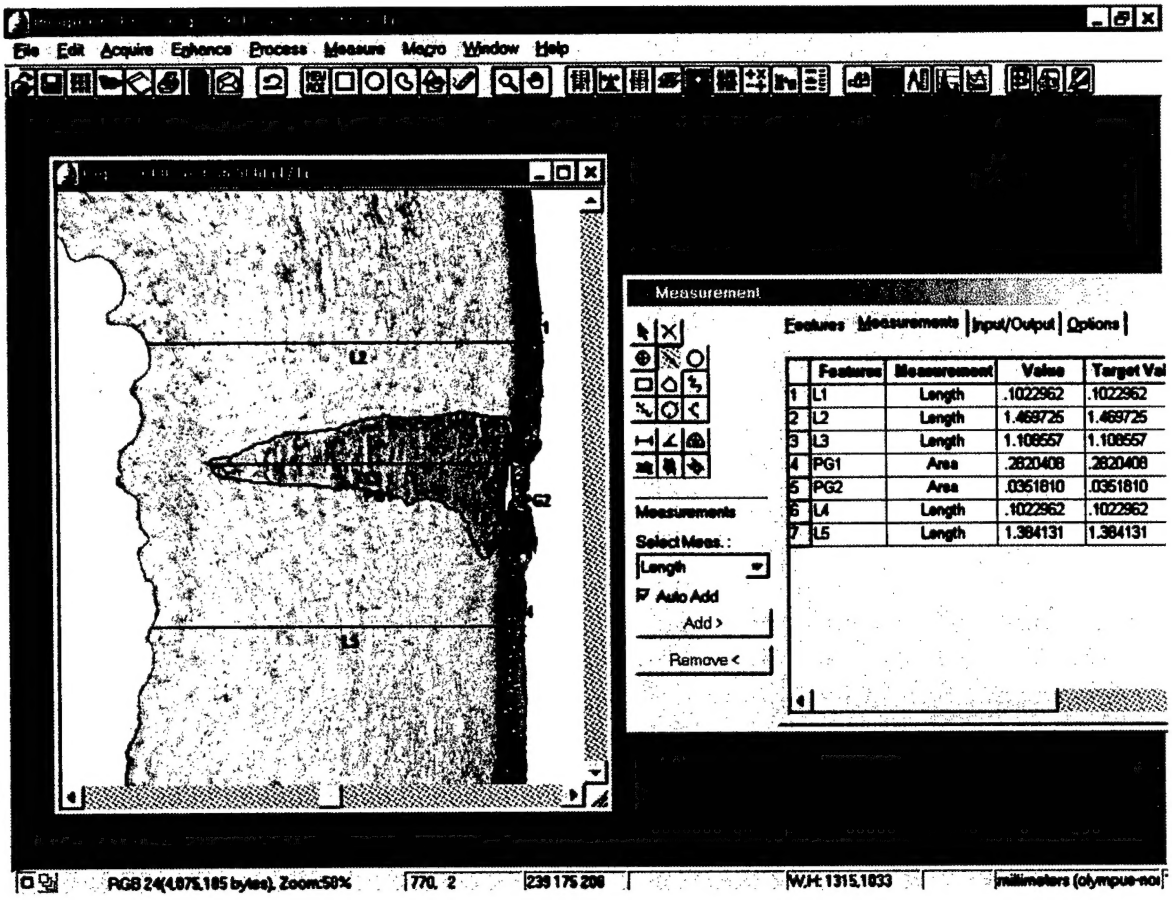

Figure 3. Screen Capture of Morphometric Data Set from a Pig Cornea Following Laser Exposure. Direct measurements of the corneal image in the left window above were made at an original magnification of 40X, using a calibration tool standardized to 0.100 millimeter. Morphometric data was recorded in the right window above. For example, the corneal epithelium measurements (L1 and L4) were both 0.102 millimeters, the depth of the corneal stromal lesion (L3) was 1.108 millimeters and the area of the corneal stromal lesion (PG1) was 0.282 mm^2.

Picosecond/femtosecond laser exposures of porcine ocular explant tissue conducted by Dr. Rockwell (Brooks AFB) produced lesions that were characterized by the formation of full thickness holes in the tissue. The lesions appeared to result from photodisruption with minimal thermal effects. Two features of the laser lesion support this position: (a) the lack of basophilic tissue staining suggests that there was no thermal degradation of the cytoplasmic proteins and (b) the melanosomes and free melanin granules swept into the laser path from the surface pigmented epithelial cells indicated significant cellular disruption (Figure 4a). The nanosecond/picosecond laser exposures of rabbit corneal equivalents conducted by Drs. Roach and Johnson (USUHS) generally induced lesions that did not result in the formation of full thickness holes in the tissue. Distinct zones of basophilic tissue staining in the direct area of the laser exposure suggested that thermal degradation of the tissue had occurred (Figure 4b).

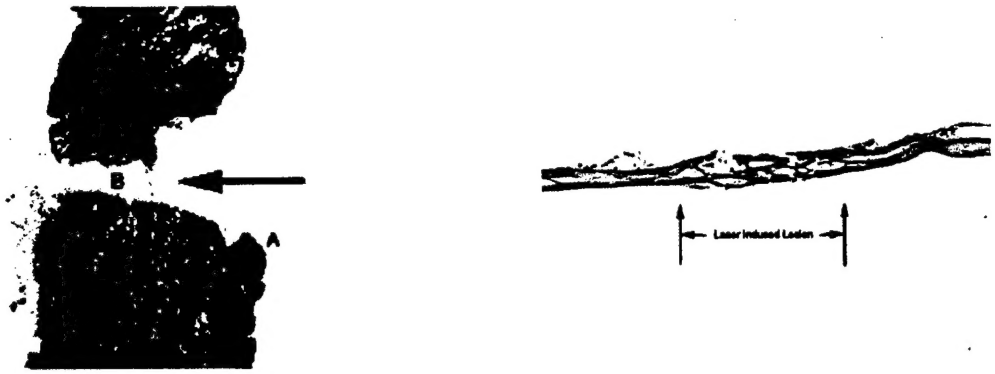

Figure 4a (left) Lesion Caused by Picosecond/Femtosecond Laser Exposure to Porcine Retinal Pigmented Epithelium Explant. Area A=Native Retinal Pigmented Epithelium on top of Choroid-Sclera. Arrow=path of laser beam. Area B=Area of laser-tissue interaction. Note the distinct hole left in the tissue and compare to the laser-tissue interaction in Figure 4b. Original magnification =160x.

Figure 4b (right) Lesion Caused by Nanosecond/Picosecond Laser Exposure to Rabbit Corneal Equivalent. Area outlined by arrows indicates laser-tissue interaction. Note the lack of a distinct hole left in the tissue and compare to the laser-tissue interaction in Figure 4a. Note the basophilic tissue staining reaction suggesting heat denaturation and coagulative necrosis. Original magnification = 60x.

Exposure of rabbit corneal tissue to millisecond pulse widths of infrared laser light produced a marked coagulative necrosis of both the epithelium and the stroma. Because the laser was operating in the millisecond pulse range, we expected to see photothermal tissue decomposition and predicted that a coagulative necrosis would occur. We also noted histologic alterations in the stromal matrix within the beam path that we interpreted as matrix remodeling. The result of the immunohistochemistry, in light of appropriate positive and negative controls, was that the MMP-2 DAB reaction product was mostly limited to the margins of the beam path (Figure 5a). In addition, the MMP-2 reaction was less intense than what we expected given the significant tissue changes in the H&E section.

Exposure of rabbit corneal tissue to the nanosecond pulse widths produced a less severe coagulative necrosis of the tissue when compared to the millisecond exposure. Nanosecond pulse widths should have less of a photothermal effect than millisecond pulse widths and be more characteristic of photomechanical tissue disruption. We believe this was why we saw less of a coagulative necrosis pattern, which is a common finding with thermal tissue damage. We noted similar stromal matrix changes in the H&E stain that we saw with the millisecond laser exposure. We found a markedly stronger immunohistochemical pattern (Figure 5b) than we would have predicted from the H&E stain with approximately half of the beam path filled with MMP-2 DAB reaction product.

It is clear from the polygonal area measurements between the two exposure conditions that the nanosecond pulse width reaction (48,200 microns^2) was greater than the millisecond pulse width reaction (30,399 microns^2). This is remarkable considering that the depth of the nanosecond lesion is considerably less (202 microns) than the millisecond lesion (378 microns). Another remarkable feature that appears to differentiate the millisecond from the nanosecond pulse widths is the keratocyte populations within the beam path. Stromal keratocytes appear normally distributed within the superficial layer of the stromal matrix contained within the beam path of the millisecond laser (Figure 5a). However, the majority of stromal keratocytes in an analogous position within the nanosecond beam path appear to be missing (Figure 5b). Although we currently do not have an explanation for this change, the lack of a necrotic cell field suggests that the keratocytes may have been removed by apoptosis.

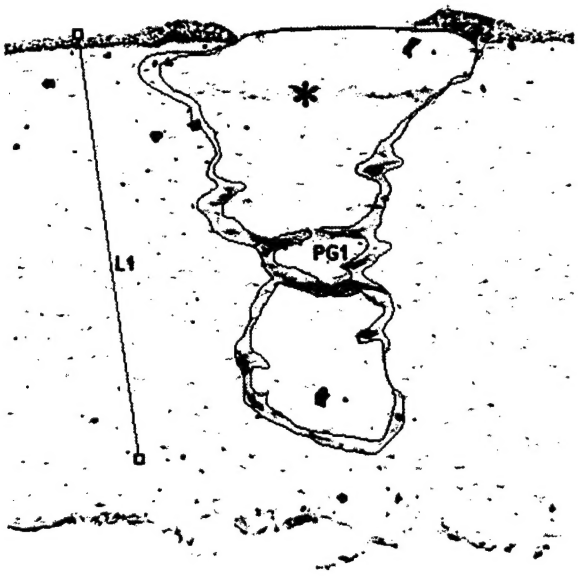

Figure 5a. Histomorphometry of MMP-2 antibody reaction following millisecond infrared laser exposure. Note normal appearing distribution of keratocytes within the upper beam path (*). L1=depth at center of lesion (line offset for better visualization of lesion)= 378 microns; PG1= area of DAB reaction product= 30,399 microns^2.

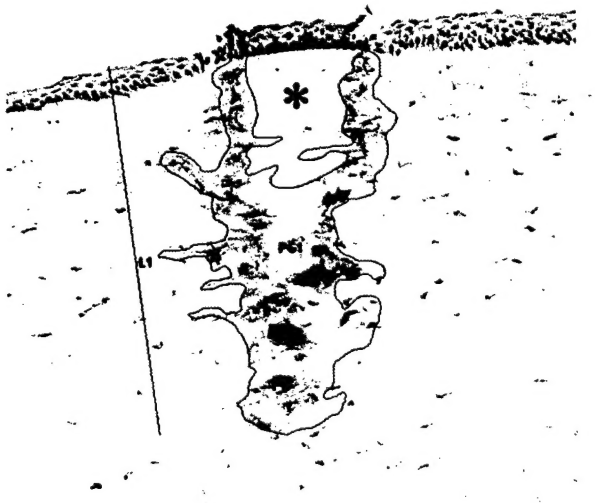

Figure 5b. Histomorphometry of MMP-2 antibody reaction following nanosecond infrared laser exposure. Note a marked absence of keratocytes within the upper beam path (*). L1=depth at center of lesion (line offset for better visualization of lesion)= 202 microns; PG1= area of DAB reaction product= 48,200 microns^2.

Personnel Supported

Dr. Thomas Eurell-P.I.
Ms. Sharon Meachum-Research Technician

I served as the research advisor for Daniel Brown, D.V.M. who is currently completing his M.S.degree. His research has been partially funded by this research grant.

Publications

D.J. Fletcher, T.E. Eurell, M.A. Mitchell, T.E. Johnson, W.P. Roach. Corneal equivalent 1540 nm laser exposure: a replacement model for *in vivo* laser exposure studies. Proceeding of SPIE Vol. 3907:69, 2000.

Eurell, TE, Johnson, T, and Roach, P. A morphometric comparison of the acute rabbit and pig corneal response to 1540 nm laser light following ex vivo exposure. Proceeding of SPIE Vol: 4246; p 180-184, 2001.

Roach, P, Eurell, TE, and Johnson, T. Corneal exposures from 1540 nm laser pulses. Proceedings of SPIE Vol: 4246; p 89-96, 2001.

An NIH proposal (NIH Assignment # 1 RO1 EY13398-01) was developed and submitted to the National Eye Institute using data obtained through collaboration with Drs. Roach and Johnson. The proposal was entitled " Effects of Infrared Laser Exposure on the Cornea".

Brown, D.R. and Eurell, T.E. Alginate as a New Biomaterial for the Growth of Porcine Retinal Pigment Epithelium. Submitted to *Veterinary Ophthalmology* and currently in review.

Interactions and Transitions

Interactions

Consultation-We reviewed our research progress with Dr. David Mattie (AL HSC\OET, WPAFB) on March 4, 1999.

I attended the Ultrashort Laser Bioeffects Workshop for AFOSR Investigators-January 26, 2000, San Jose, CA. We reviewed the status of research projects among several AFOSR investigators working on laser-tissue interaction.

Site visit with Drs. Roach, Johnson and Kozumbo at Dr. Eurell's laboratory-August 23-25, 2000. I reviewed the various analytical procedures we use to study laser-ocular tissue interaction.

I attended the Ultrashort Laser Bioeffects Workshop for AFOSR Investigators-January 25, 2001, San Jose, CA. We reviewed the status of research projects among several AFOSR investigators working on laser-tissue interaction.

Transitions

None-all transfers have involved collaboration with colleagues.